6-2002

# The optimization of sol-gels as sensing arrays and the testing of sol-gel precursors through the use of fluorescence measurements of eosin-y

Rachel M. Bukowski
*Union College - Schenectady, NY*

# THE OPTIMIZATION OF SOL-GELS AS SENSING ARRAYS

and

# THE TESTING OF SOL-GEL PRECURSORS THROUGH THE USE OF FLUORESCENCE MEASUREMENTS OF EOSIN-Y

By

Rachel M. Bukowski

**********

Submitted in partial fulfillment

of the requirements for the degree

of Bachelor of Science

UNION COLLEGE

March, 2002

# Abstract

BUKOWSKI, RACHEL M. The Optimization of Sol-Gels as Sensing Arrays and The Testing of Sol-Gel Precursors Through the Use of Fluorescence Measurements of Eosin-Y. Union College. Department of Chemistry, Winter 2002

The purpose of the first project, performed in collaboration with Professor Frank Bright of SUNY at Buffalo, was to optimize the conditions and variables for a Cartesian Technologies Pinprinter to print reproducible spots of sol-gels doped with Ruthenium Diphenylphenathrene ($Ru(dpp)_3^{2+}$), an oxygen-sensing complex, on microscope slides. We attempted to optimize these variables by 1) the alteration of the printing speed of the sol-gel microarrays, 2) variation of the drying temperature of the gels after they had been printed, 3) controlling the reaction rate of the sol-gel, and 4) various methods of slide pre-treatment. We found that a print speed of 10-25ms, drying the sol-gels at room temperature and no spin-coating over the microarrays were the most optimal results, and the resulting microarrays could be employed for analytical chemistry research purposes.

The primary purpose of the second project was to create an effective pH sensor through the use of Eosin-Y within a sol-gel monolith matrix. The most effective precursor(s) must meet the criteria of adherence to a linear plot of fluorescence intensity versus concentration of encapsulated Eosin-Y, reversibility of the sensing capabilities as close to 100% as possible, and minimal cracking in the monolith. The precursors tested were TMOS, TEOS, n-propyl TMOS/ TMOS, methyl-TMOS/ TMOS and phenyl TEOS/ TEOS. It was found that the ormosils n-propyl TMOS/TMOS and methyl TMOS/ TMOS yielded the most effective sensors, overall. The use of Eosin-Y as an indicator for reaction rate of the sol-gel was also explored, as its emission spectra shifts when the ratio of water to ethanol in the solvent is varied.

## Acknowledgements

I would first like to thank the Union College Chemistry Department and its faculty for providing me with an excellent education and the tremendous opportunity to perform this research. The Union College Summer Research Fellowship and the Union College Internal Education Fund also aided substantially in my research.

I would also like to thank Professor Mary Carroll for her advisement through this thesis and throughout my college career. Her guidance has helped me tremendously, and I am truly grateful for this.

Many thanks to Professor Frank Bright, his research group and the students and faculty at SUNY Buffalo for an insightful and meaningful glimpse into research and graduate school life over the Summer of 2001...see you in June!

To all my fellow Chem majors: thanks for all the laughs, all the memories, all those late nights in the MM Lab, all those cups of coffee...best of luck to all of you in the future, I'll miss you guys.

To the friends I have made at Union College over the last four years: You have shaped me into the person I am today, let's hope the good times don't end after graduation. "I hope it was okay, I know it wasn't perfect. I hope in the end we can smile and say it was all worth it". ~Ani DiFranco

Lastly, I would like to thank my family, especially my father, mother and sister. I would not be where I am today if it was not for your endless support and love.

Rachel M. Bukowski

Rachel M. Bukowski

TABLE OF CONTENTS

## TABLE OF FIGURES

## TABLE OF TABLES

# INTRODUCTION

# Introduction

## A. Introduction to Sol-Gels

A sol-gel is a silicon oxygen matrix formed by means of a combination hydrolysis and condensation reaction at room temperature. It utilizes semi-metal alkoxide monomers such as tetramethoxysilane (TMOS), tetraethoxysilane (TEOS) and derivatives of these two. The hydrolysis reaction tends to be on the order of a couple of hours depending on preference of viscosity of the gel. However, it takes approximately two weeks for the gel to form a solid piece of glass, or "xerogel".

The first step of the reaction is the formation of the "sol", when water causes silanol [Si-OH] groups to form [1]. After the formation of Si-OH groups, the deprotonation of the silanol groups and the condensation and polycondensation to form Si-O-Si bonds occurs [1]. Following the bonding of the Si-O-Si groups, a three-dimensional matrix, the "gel", is formed with the introduction of an acid catalyst [1]. HCl was the catalyst used in all of the experimental procedures involving the preparation of sol-gels. The formation of the gel includes two different processes: the development of a wet gel, which, as discussed earlier, occurs on the order of a couple hours, and ethanol and water evaporation to form a xerogel, which occurs on the order of a couple days [1]. The following is a representation of the sol-gel process [2]:

$Si(OR)_4 + nH_2O \rightarrow Si(OR)_{4-n}(OH)_n + ROH$ *hydrolysis*

$Si\text{-}OH + RO\text{-}Si \rightarrow Si\text{-}O\text{-}Si + ROH$ *condensation*

$Si\text{-}OH + HO\text{-}Si \rightarrow Si\text{-}O\text{-}Si + H_2O$ *polycondensation*

The Si-O matrix formed in this process is suitable for the entrapment of chemical species, including biological species, indicators, dyes and sensors. This gives a number of

advantages over the immersion of similar species in an aqueous environment, as the methods of immersion of an indicator in an aqueous environment often interfere with the indicator's chemistry.

A number of studies have been performed [2,3,5] in which organic molecules have been introduced into the polycondensation reaction at varying times during the reaction, and as a result have been encapsulated in the sol-gel matrix. Since the environment of the matrix is relatively inert, and the pores in the sol-gel are relatively large, the organic molecule is allowed to rotate freely once it has become entrapped [1]. Therefore, the sol-gel matrix provides a nearly ideal environment for the entrapment of indicators such as Eosin-Y for sensing purposes. Small analytes can infiltrate the sol-gel matrix without destroying it or altering its chemical composition, and can thus interact with the indicator.

Methods of indicator immobilization in sol-gel include impregnation, covalent binding and chemical doping [4]. Impregnation refers to physical or chemical adsorption on the preformed glass. Covalent binding is the most efficient method, and refers to the linkage of the dye to a suitable matrix [4]. Chemical doping is the most popular method and refers to the incorporation of the indicator or reagent during the formation of the sol-gel glass [1].

Figure 1 provides a visual simulation of the entrapment of a biological molecule into the forming sol-gel matrix. The protein to be encapsulated is added to the sol after partial hydrolysis of the precursor(s) [3]. This process nearly ensures an even and homogenous distribution of the biomolecule.

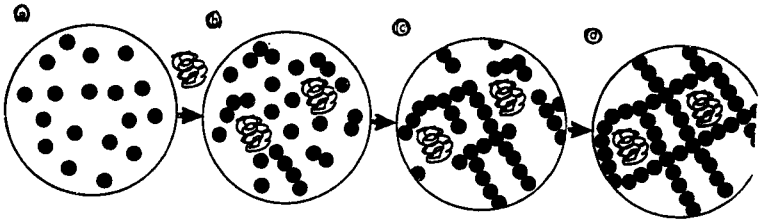

**Figure 1: Entrapment of a Protein into Sol-Gel Matrix**
***Reprinted from* [3]**

Inorganic supports, particularly silica-based matrices, offer several advantages over organic polymer supports, including physical rigidity and high abrasion resistivity; negligible swelling in both aqueous and organic solutions, chemical inertness, and excellent optical transparency and low intrinsic fluorescence [1]. Another advantage of entrapment in a sol-gel matrix over entrapment in an aqueous environment is that proteins and other biological molecules often fail to retain their native stabilities and reactivities upon immobilization in the aqueous environment. This is a flaw that results in low stabilities and altered functional responses of biosensors incorporating them [3]. Sol-gels can provide a host matrix for biomolecules; those immobilized by this method retain their functional characteristics to a large extent [3]. It has also been demonstrated that the sol-gel matrix prevents self-aggregation and microbial attack.

As a result of the sol-gel's ability to encapsulate a number of biological materials, sol-gel sensors can be used for biomedical applications, such as sensing dissolved oxygen in the blood and high levels of nitric oxide (NO) [3].

Sol-gel sensors can be prepared in a number of physical configurations. The sol-gel can conform to various shapes and sizes because of its large range of viscosities and its unique chemical composition. A monolith is a solid piece of sol-gel whose reaction has run to completion. It has taken the form of the container (ie: cuvette) that it has been allowed to solidify and shrink in. The pH sensors described in this thesis are in monolith form. Sol-gels can also be formed into microarrays. Optimization of microsensor-to-microsensor reproducibility and function was the focus of the work performed by this author at SUNY Buffalo. Additionally, sol-gels can form thin films that are less than 1 μm in thickness. With the use of a spin-coater, sol-gel thin films can be spread over a variety of surfaces, including glass.

## B. Ormosils

Ormosils are sol-gels that have been modified by changing the precursor from TMOS or TEOS to a precursor with organic substituents such as phenyltriethoxysilane or methyltrimethoxysilane. By using ormosils, sensor performance is enhanced because the interface of the sensor becomes increasingly hydrophobic [5], and reaction rate is increased as a result of increasing polycondensation of Si-OH groups [6]. In this thesis, I describe the results of experiments using ormosils and TEOS or TMOS as a platform for Eosin-Y based pH sensors.

Figures 2, 3, 4, 5 and 6 represent the structures of the precursors used in the experiments described in this thesis

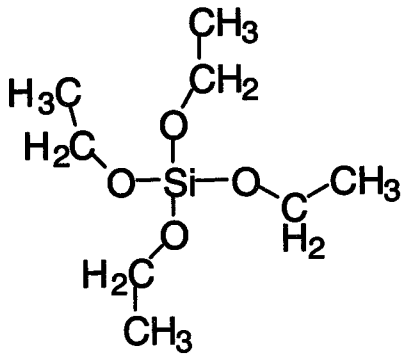


**Figure 2: Tetraethoxysilane (TEOS)**

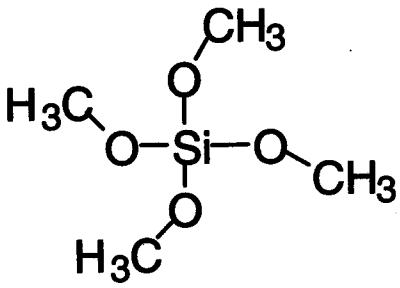


**Figure 3: Tetramethoxysilane (TMOS)**

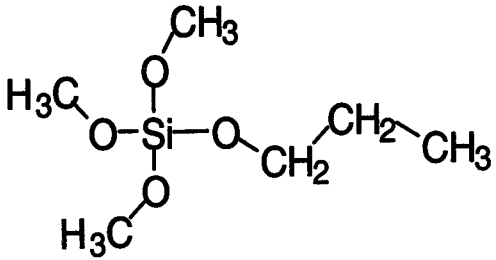


**Figure 4: n-Propyltrimethoxysilane (n-Propyl TMOS)**

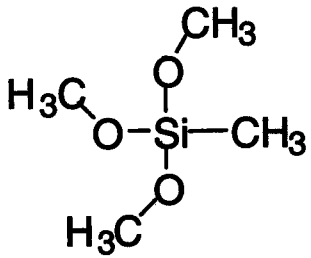


**Figure 5: Methyltrimethoxysilane (Methyl TMOS)**

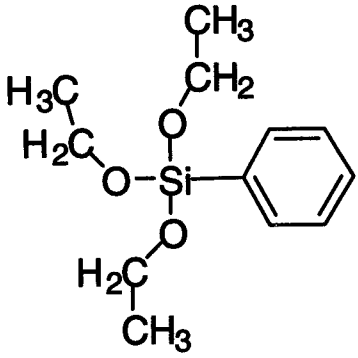


**Figure 6: Phenyltriethoxysilane (Phenyl TEOS)**

In the set of experiments performed at Union College, the goal was to take these five precursors and see which gave a superior response upon encapsulation of Eosin-Y, a fluorescent pH indicator. The monoliths were assessed based on the adherence to linearity of fluorescence as a function of concentration of the encapsulated Eosin-Y, the response of the Eosin-Y to changes in pH and the overall appearance and structural integrity of the monolith after solvent and water evaporation.

## C. Fluorescence Principles

The use of fluorescence measurements to ascertain information about the microenvironment of the sol-gel was an integral component to all of the experiments performed. Fluorescent probes can be incorporated into sol-gel-derived materials at very low levels ($<10^{-6}$ M) and thus do not alter the overall properties of the material [7]. The combination of time-resolved and steady-state fluorescent techniques makes it possible to determine the average microenvironment of a probe [7].

The fluorescence of a molecule can be attributed to its excitation to a higher energy level than its lowest-energy ground state configuration, and its return back to this ground state. The return of an electron to the lower energy orbital ultimately causes the molecule to emit a photon (fluoresce). The amount of fluorescence intensity emitted by a sample is directly related to the concentration of the fluorescing species if the samples are low-absorbing and the absorbance is less than 0.05. Thus we can expect that fluorescence intensity will be linear in relation to analyte concentration if the samples prepared have an absorbance less than 0.05.

Figure 7 represents a Jablonski diagram, which is often used to explain the principles of fluorescence spectroscopy.

The quenching of fluorescence, which was used in the work done at UB and presented in Project I, has traditionally been used to study probe accessibility, translational mobility and conformational flexibility of the microenvironment of the sol-gel matrix. Emission wavelength, which was used in the work performed at Union College and presented in Project II, has traditionally been used to study the internal

polarity, surface silanol content, solvent composition and pH of the microenvironment of the sol-gel matrix [7].

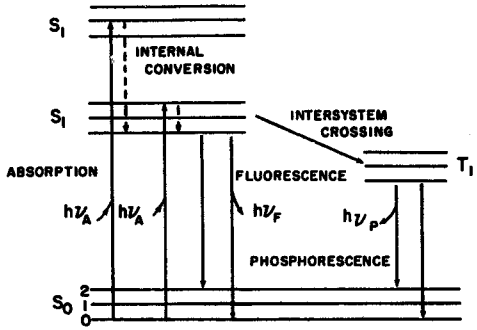


Figure 1.3. Jablonski diagram.

**Figure 7: Jablonski Diagram**
***Reprinted from*** **[8]**

## D. Indicators

There were two indicators used in these experiments, ruthenium diphenylphenathrene ($Ru(dpp)_3^{2+}$) and Eosin-Y. The $Ru(dpp)_3^{2+}$ was used in the microsensor experiments conducted at the University at Buffalo, and the Eosin-Y was used in the monolith experiments conducted at Union College.

The structure of ruthenium diphenylphenanthrene can be seen in Figure 8:

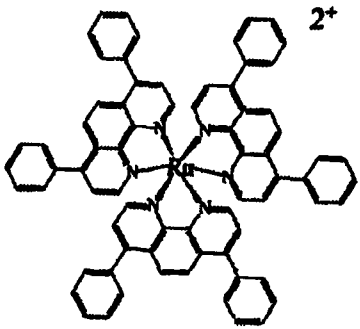


**Figure 8: Structure of $Ru(dpp)_3^2$**
***Reprinted from* [9]**

Ruthenium diphenylphenanthrene is a highly fluorescent complex that is a dark orange color in solution. The sol-gels used to print microarrays of spots were doped with this Ruthenium complex. This complex was chosen because it absorbed at 488 nm and was therefore ideal to use in conjunction with the argon-ion laser used to excite the

fluorescence of each printed spot. Moreover, ruthenium diphenylphenanthrene can be used to sense low levels of oxygen gas. The ruthenium complex is highly fluorescent, and when it comes in contact with $O_2$, its fluorescence is quenched. When oxygen gas is displaced by another gas, such as nitrogen, the entrapped ruthenium complex returns to its original fluorescence intensity.

The sol-gel matrix, since it is composed of silicon and oxygen, carries a slightly negative charge. Since the ruthenium complex carries a 2+ charge, it will not leach out of the matrix, as negative ions might, once it [illegible]apsulated within the matrix.

The structure of Eosin-Y can be viewed in Figure 9:

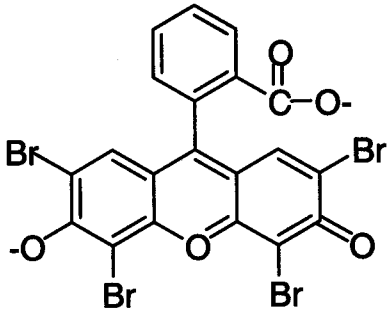


**Figure 9: Structure of Eosin-Y [10]**

Eosin-Y is an orange-colored pH-sensitive dye. It is excited at 514 nm and emits at roughly 540 nm; however, it was found that the fluorescence behavior of Eosin-Y

varies based on the polarity of the solvent it is dissolved in. As the polarity of the solvent decreases, the wavelength at which the Eosin-Y experiences its peak fluorescence intensity increases as well.

The absorption spectrum of Eosin-Y can be found in Figure 10:

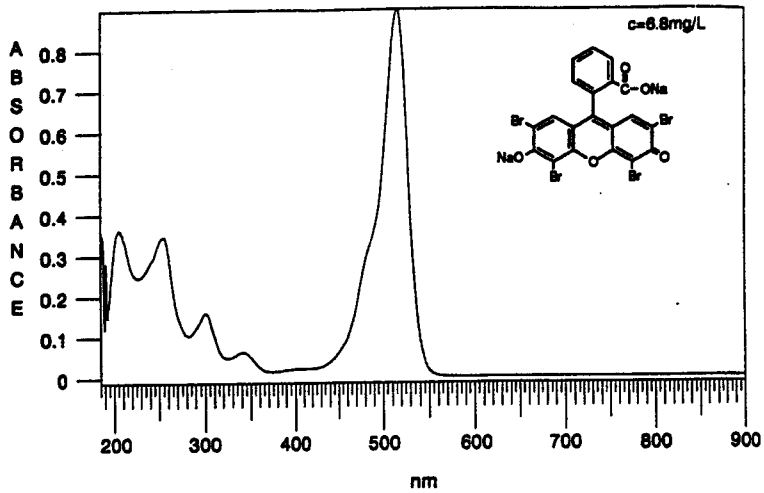


**Figure 10: Absorption Spectrum of Eosin-Y**
***Reprinted from* [10]**

At a pH greater than 3.00, Eosin-Y exhibits fluorescent properties which are greatly reduced when the pH of the solution the Eosin-Y is exposed to is lowered below 3.00. As one can infer by viewing the structure of Eosin-Y, this molecule contains a carboxylic acid group and a hydroxyl group, which have pKa values of 3.25 and 3.80, respectively [11]. The addition of acid to the solution protonates these groups and thus, changes the chemical composition of the Eosin-Y. This changes the molecular structure of the molecular species. However, by raising the pH and deprotonating the carboxyl and hydroxyl groups, the fluorescence intensity of the Eosin-Y is increased. Although Eosin-Y carries a negative charge in the sol-gel solutions, there has been no evidence of leaching of Eosin-Y from the monoliths.

# PROJECT I:
# THE OPTIMIZATION OF SOL-GELS AS SENSING ARRAYS

# PROJECT I
# CHAPTER 1:
# EXPERIMENTAL

## Chapter 1: Experimental

### *A. Instrumentation Used*

Although I learned how to operate a number of complex instruments in the Bright Lab, including an SLM 48,000 Spectrophotometer and Nitrogen Dye Laser, the three main instruments utilized in this research were a Cartesian Technologies Pinprinter, an Argon-Ion Laser and a CCD Camera. The pinprinter was used to print the microarrays of sol-gel spots doped with Ruthenium Diphenylphenathrene ($Ru(dpp)_3^{2+}$).

The Argon-ion laser was used to excite these spots at 488 nm and the spots were then magnified 40x with a microscope. They were then viewed with a Charge Coupled Detector (CCD) Camera and Projected onto a PC screen in color. A diagram of this apparatus is shown in Figure 11:

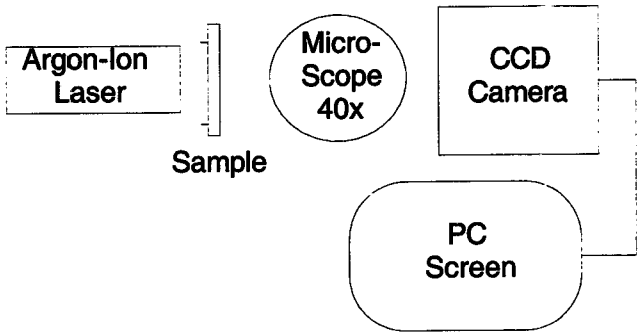


**Figure 11: Rough Diagram of Imaging Apparatus**

### *B. Background*

In order to obtain reproducible sol-gel spots, there were two major components of the printing process that needed to be addressed. First, the gel was evolving as the printing was taking place, and the spots were becoming smaller as the printing progressed because the gel was becoming more viscous. Eun Jeong Cho, a graduate student at the University at Buffalo, is currently performing experiments in which she adds surfactants to the evolving sol-gel in an attempt to slow the reaction while the printing is progressing.

Another aspect of the printing process that needed to be addressed was the preparation of the surface of the glass slides on which the spots were being printed. It appeared that the spots were not adhering properly to the surface of the slide and this was causing them to become nonuniform. The standard procedure for slide preparation was a 15-minute treatment with 1-M NaOH and then a roughly 1-minute wash with ethanol. This process created a highly polar surface for a polar sol-gel spot to adhere to, and it is possible that the sol-gel spots were spreading out too much upon being printed onto the slides. On the other hand, if a nonpolar solvent is used to wash the slides, then the spots placed on the slide would bead up too much and result in too much density in the center of the spot and an unstable sol-gel sensor. To address these problems, a new slide preparation method was used that involved treating the slides with amino-propyltriethoxysilane (APTES), a sol-gel precursor. Because APTES has both a polar and nonpolar component, it was expected that sol-gel spots would be neither too spread out nor too small on APTES-treated slides.

The structure of APTES is shown below:

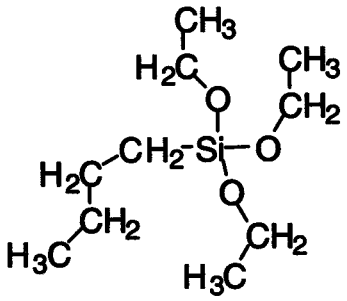

**Figure 12: Structure of APTES**

The spots were also dried at varying temperatures, and a spin-coated sol-gel layer was placed over some of the spots in order to determine which factors would account for the most uniform spots.

## *C. Experimental Procedures*

### 1. APTES Experiments

The following instruments and chemicals were used in this set of experiments:

| |
|---|
| Amino-propyltriethoxysilane, United Chemical Companies, Inc. |
| Triethylamine, Aldrich Chemicals (99.5%) |
| Toluene, Aldrich Chemicals (99.8%, Anhydrous) |
| Chloroform, Aldrich Chemicals (99+%) |
| Acetone, J.T. Baker (99.5%) |
| Methanol, Fisher Chemicals (99.9%) |
| 100 mL TEKK Graduated Cylinder |
| 5 mL, 1 mL Ranin Pipettes |
| 25 μL Eppendorf Pipette |

The first series of experiments involved the use of APTES to modify the surface of the slides so it would be neither extremely polar, nor extremely nonpolar.

The slides were treated in the following fashion [12]:

Toluene, APTES and triethylamine were combined in a 1:0.02:0.01 molar ratio in a beaker and the desired amount of slides were placed in the beaker, with enough solution to completely cover the slides. The beaker was covered with parafilm to minimize exposure to the air. Argon gas was passed through the solution for 10 minutes in order to rid the container of any oxygen or moisture. After the argon gas was passed through the solution, the slides were allowed to sit overnight. The following day, the slides were washed three times in succession with chloroform, acetone and methanol, and then dried in a stream of argon gas. At this point, the slides were prepared for the printing process.

A sol-gel solution was made using tetraethoxysilane (TEOS), ethanol, water and HCl in a $1:2:2:10^{-4}$ molar ratio, and this solution was stirred on a stirring plate and allowed to

hydrolyze for 2 hours. After 2 hours, 100 μL of a 22-mM solution of $Ru(dpp)_3^{2+}$ was added to the gel. The spots were printed on the slide in a 10x10 microarray, and each spot had a diameter of approximately 100 μm. A 10-25ms print speed [see explanation on following page] was used to print the spots, and they were allowed to dry for a week. After the spots dried, they were imaged using the device in Figure 11, and a response profile for nitrogen and oxygen gases was taken for each slide.

## 2. Print Speed, Drying Temperature and Spin-Coating Experiments

The second set of experiments involved varying a number of different factors in the printing and treatment of the sol-gel spots in order to find the most optimal set of printing conditions for the sensors. The printing speed and drying temperature of the spots was varied from slide to slide, and a layer of sol-gel was spin-coated over some of the spots in order to determine if this layer would prevent cracking within the spots after they had dried. The numbers 1-20 represent the number of slides treated in this experiment and the other columns represent how each particular slide was treated. The general experiment is outlined in Table 1:

| 10-25ms | 25-50ms | 5-10ms | 5-5ms | 1st Drying | Spin Coating? | 2nd Drying |
|---|---|---|---|---|---|---|
| 1 | 2 | 3 | 4 | Room temp | yes | Room temp |
| 5 | 6 | 7 | 8 | Room temp | no | N/A |
| 9 | 10 | 11 | 12 | 4 degrees C | yes | 4 degrees C |
| 13 | 14 | 15 | 16 | 4 degrees C | yes | Room temp |
| 17 | 18 | 19 | 20 | 4 degrees C | no | N/A |

**Table 1: Outline of Experimental Procedure 2**

The numbers 10-25ms, 25-50ms, 5-10ms and 5-5ms represent the different print speeds used in the experiment (in milliseconds). The first number is represents the speed of the pin as it moves from spot to spot; 5 is a relatively slow speed, 25 is relatively fast. The second number represents the amount of time the needle is in contact with the slide in milliseconds. The slides were dried at varying temperatures after printing and after

spin coating. After the initial printing, they were dried at either room temperature or 4°C, and after the spin coating was added, they were either dried at room temperature or 4°C.

In this experiment, we did not pre-treat the slides with APTES because it is so time-consuming. Slides were treated with 1 M NaOH for 15 minutes, washed with Ethanol and dried under a stream of argon gas.

Each of these slides was prepared using the following sol-gel recipe for the spots:

- 3.345 mL TEOS
- 1.700 mL Ethanol
- 0.540 mL Water
- 15 μL 0.1 M HCl

The sol-gel was then put on a stir plate and stirred for 3 hours to hydrolyze. It was subsequently doped with 80 μL of 11 mM $Ru(dpp)_3^{2+}$ and the first four slides were printed using the different printing speeds. A new sol-gel solution was made every day to print four new slides, until slides 1-20 had been printed out at the appropriate speeds.

Following the printing of the spots, the slides were covered so as not to expose the spots to the light, and they were stored at the appropriate temperatures. After one week of drying, the spin-coated layer was placed on the appropriate slides (1-4, 9-12 and 13-16) and these slides were allowed to dry for an additional week.

To spin-coat a sol-gel layer over an array of spots, the following procedure was employed: a new sol-gel solution was made using the same recipe that was used to make the sol-gel for the spots, except that no Ruthenium complex was added to this one. The slide was cut on the sides to form a small square, and the slide was then taped to an Analytical Chemistry Spin-Coater. 20 μL of the new sol-gel solution was pipetted over the dried microarray, and the spin-coater was run at 3000 rpm for 30 seconds. After 30 seconds, it was safe to assume that the spots were sufficiently coated with the gel.

After all of the slides had been prepared and dried, they were imaged using the CCD Detector. When imaging the spots, the following procedure was used to determine the reproducibility of the spot-to-spot images: take the fluorescence intensity at 100% Nitrogen gas and divide it by the intensity at 100% Oxygen gas, then determine the average of this intensity ratio, the standard deviation and the relative standard deviation. Our goal was a relative standard deviation of < 5%.

## 3. Print Speed Experiments

The following instruments and chemicals were used in this set of experiments:

| |
|---|
| APTES, United Chemical Technologies, Inc. |
| Triethylamine, Aldrich Chemicals (99.5%) |
| Toluene, Aldrich Chemicals Inc. (99.8%, anhydrous) |
| N-Propyl-trimethoxysilane, United Chemical Technologies, Inc. |
| Tetramethoxysilane, United Chemical Technologies, Inc. |
| Corning Glass Microscope Slides |
| 1 mL Ranin Pipette |
| 20 μL Eppendorf Pipette |

It was determined that further experiments should be performed on the manipulation of printing speeds of the pinprinter in order to optimize the reproducibility of the size and composition of the spots. Slides were treated with APTES for this set of experiments, since the most optimal results needed to be obtained and APTES is a more effective pretreatment for the spots than NaOH. A device was used that allowed us to treat 20 slides at once with APTES, and this made for a less time-consuming pre-treatment of the slides. Once the slides had been rinsed and had finished drying, they were placed in a cardboard box to keep them away from light and minimize their exposure to air currents.

A new recipe was used to make the sol-gel solution for these spots because the old recipe took approximately 2-3 hours to hydrolyze. Hydrolysis occurred in one hour when we used this new recipe. This particular solution has been shown to crack less than the TEOS sol-gels [13]. The recipe is as follows:

- 0.5 mL tetramethoxysilane (TMOS)
- 0.5 mL n-Propyl-trimethoxysilane (n-Propyl TMOS)
- 1.2 mL Ethanol
- 0.36 mL Deionized Water
- 0.04 mL 1 M HCl

After one hour of stirring, 3 μL of 25 mM $Ru(dpp)_3^{2+}$ was added to the solution, and the slides could be printed. One APTES-treated slide was used for each particular print speed that was programmed into the pinprinter's computer, and the following speeds were used to print the microarrays:

| | | |
|---|---|---|
| • 10-10ms | • 10-15ms | • 10-20ms |
| • 10-25ms | • 15-15ms | • 15-20ms |
| • 15-25ms | • 20-20ms | • 20-25ms |

Based on the previous set of experiments, it was known that printing at very slow speeds such as 5-5ms and 5-10ms and very high speeds such as 25-50ms would yield unusable data, so these speeds were not included in this particular set of experiments. At very slow speeds, the spots were square-shaped, rather than round, and very small. At very fast speeds, the spots were too large and ran into one another.

After the microarrays had been printed, the slides were stored at room temperature in a covered cardboard box so that light could not filter in. They were then imaged with the argon-ion laser and CCD camera, and the sensors' spot-to-spot reproducibility was evaluated.

# PROJECT I
# CHAPTER 2:
# RESULTS

# Chapter 2: Results

## A. APTES Experiments

Microarrays of sol-gels doped with the Ruthenium complex were printed on slides pre-treated with APTES. They were then imaged in the CCD camera, and the response profiles of the slides were taken. A response profile consists of flooding the chamber containing the microarray with nitrogen gas ($N_2$) and taking fluorescence intensity readings roughly every 30 seconds for about 2-3 minutes. After the intensity readings have leveled off, the chamber is then flooded with oxygen gas ($O_2$) and fluorescence intensity readings are again taken every 30 seconds until they level off. This procedure is repeated 3-5 times.

The purpose of the response profile is twofold. The first purpose is to determine how well the microarray is responding to changes in concentration of nitrogen and oxygen gas, since the Ruthenium complex's fluorescence is quenched by oxygen. If the microarray responds to oxygen, then a microsensor has been made successfully. The other purpose of the response profile is to determine whether or not photobleaching is occurring in the sensor because of the laser intensity. When the fluorescence intensity is taken at 100% $N_2$, after being quenched by $O_2$, that intensity is sometimes lower than the first time the intensity was measured at 100% $N_2$. When this phenomenon occurs one can safely assume that photobleaching of the Ruthenium complex has occurred.

Figures 13 and 14 are the response profiles of the microarrays of the slides pre-treated with APTES.

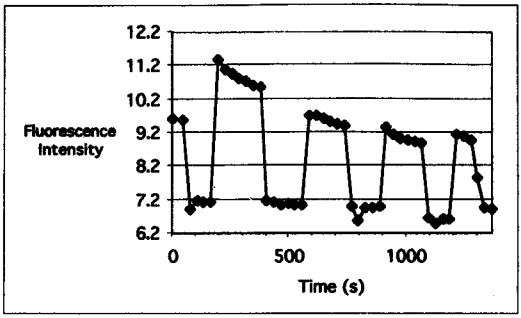


**Figure 13: Response Profile of APTES-treated Slide 1: Sol-gel Microarray Doped with Ruthenium Complex**

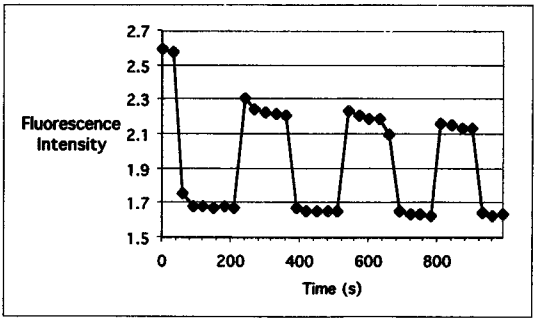


**Figure 14: Response Profile of APTES-treated Slide 2: Sol-gel Microarray Doped with Ruthenium Complex**

**Peaks on Response Profile: 100% $N_2$**
**Valleys on Response Profile: 100% $O_2$**

## B. Print Speed, Drying Temperature and Spin-Coating Experiments

It is important to note that among the data collected for this particular set of experiments, the only print speed employed that produced usable data was 10-25ms. The 25-50ms print speed was so fast that all of the spots were too large, approximately 120 μm, and they ran together. The 5-5ms and 5-10ms print speeds were so slow that the spots were not even round, but they were in the shape of small rectangles instead. In addition to this, the pin on the pinprinter would often clog before the microarray had been fully printed due to the slow speed of the printing and the evolution of the sol-gel during this time. The sol-gel would, in fact, become so viscous that the pin was unable to print the spots towards the end of the microarray. This concept can be illustrated in Figures 15, 16, 17 and 18, which contain the images of the sol-gel microarrays printed at different speeds, excited with the laser, detected with the CCD camera and imaged on the computer screen.

In the microarrays using the 5-5ms and 5-10ms print speed, it is difficult to see that the spots are growing smaller towards the end of the microarray, since the spots are all so small. However, in the microarrays using the 10-25ms and 25-50ms print speed, it is easy to see. In these two images, one can see that as the pinprinter moves from left to right, the spots grow increasingly smaller.

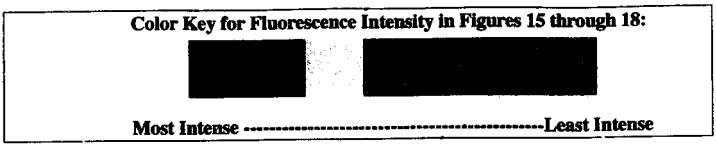


**Figure 15: Image of Sol-gel Spots Printed at 5-5ms**
**Diameter of 1 spot = ~80 μm**

**Figure 16: Image of Sol-Gel Spots Printed at 5-10ms**
**Diameter of 1 spot = ~80 μm**

**Color Key for Fluorescence Intensity of Figures 15 through 18:**

**Most Intense ----------Least Intense**

**Figure 17: Image of Sol-gel Spots Printed at 10-25ms**
**Diameter of 1 spot = ~100 μm**

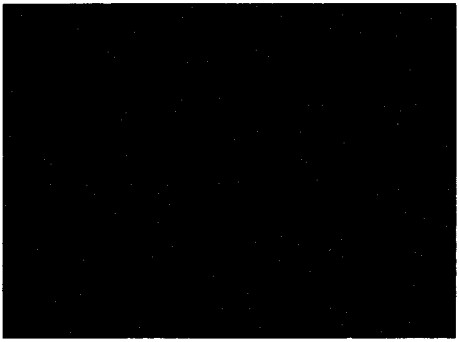

**Figure 18: Image of Sol-gel Spots Printed at 25-50ms**
**Diameter of 1 spot = ~120 μm**

An interesting observation was recorded in regards to the drying temperature of the microarrays. The fluorescence of $Ru(dpp)_3^{2+}$ in the slides that were dried at 4°C seemed to have been quenched. When the arrays were excited with the laser beam and imaged with the camera, their spot intensities were almost negligible; the excited spots could barely be seen.

Although the spin coating was effective in preventing the spots on the microarray from cracking, it hindered the sensing capabilities of the ruthenium complex encapsulated inside the sol-gel matrix, as one can see by referring to Figure 19 and comparing it to Figures 13 and 14. The response time of the ruthenium complex encapsulated inside the sol-gel has been significantly raised, as the nitrogen and oxygen gases must first infiltrate the Si-O matrix in the spin coating, then the Si-O matrix of the pinprinted spots. This data is much noisier than the previous response profile taken, so the two cannot be compared directly; however, it is quite obvious that despite this, the response time has been raised.

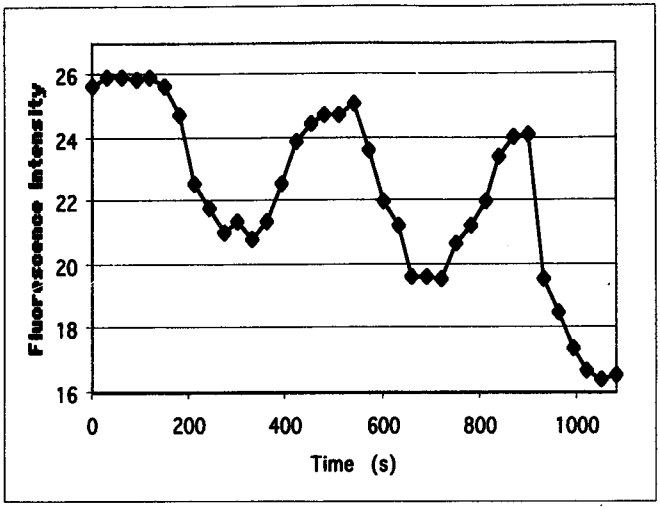


**Figure 19: Response Profile of Sol-Gel Microarray Doped with $Ru(dpp)_3^{2+}$ With Spin-Coated Sol-Gel Layer Cover**

One can also refer to Figures 20, 21, 22 and 23 to see a visual comparison of the images of two different microarrays. One of the microarrays has a spin-coated sol-gel layer over it and the other microarray does not. These figures show each microarray at 100% $N_2$ and 100% $O_2$, and the differences between the two are evident, as the contrast on the microarray without the spin-coating is far more apparent than the contrast on the microarray with the spin-coating.

100% $N_2$

**Figure 20: Spots with Spin Coating at 100% $N_2$**

100% $O_2$

**Figure 21: Spots with Spin Coating at 100% $O_2$**

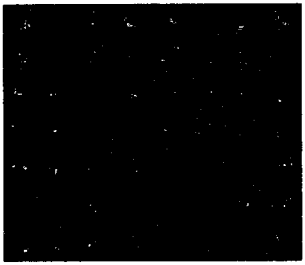

**Figure 22: Spots without Spin Coating at 100% $N_2$**

**Figure 23: Spots without Spin Coating at 100% $O_2$**

**Color Key for Fluorescence Intensity of Figures 15 through 18:**

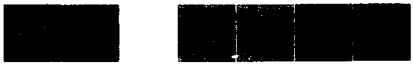

**Most Intense ----------Least Intense**

## C. Print Speed Experiments

Although the final set of experiments was unable to be concluded due to a broken computer on the CCD camera, results that were quite useful were still obtained. A number of printing speeds were tested in order to determine which speed yielded the most reproducible spots. Of the speeds previously listed, reproducibility was determined for the following speeds:

- 10-10ms
- 10-15ms
- 10-25ms
- 20-20ms
- 15-25ms
- 10-20ms

Unfortunately, I was unable to obtain data for 15-15ms, 15-20ms and 20-25ms print speeds.

Table 2 displays the average intensity of $N_2/O_2$ of each spot, the standard deviation from the average, and the relative standard deviation for each particular printing speed studied and analyzed.

| Print Speed | Ave. Intensity | SD(+/-) | RSD |
|---|---|---|---|
| 10-10ms | 2.32 | 0.18 | 8% |
| 10-15ms | 3.20 | 0.44 | 14% |
| 10-20ms | 3.07 | 0.41 | 13% |
| ***10-25ms*** | ***3.44*** | ***0.18*** | ***5%*** |
| 15-25ms | 5.69 | 0.43 | 8% |
| 20-20ms | 3.62 | 0.36 | 9% |

**Table 2: Summary of Data from Print Speed Experiments**

As one can infer from Table 2, 10-25ms appears to be the optimal printing speed, as it gave the lowest relative standard deviation of spot-to-spot reproducibility at 5%. The only other printing speeds that came close to this very low RSD were 10-10ms and 15-25ms, each having an RSD of 8%. Figures 24, 25, 26, 27, 28 and 29 are the individual graphs of each printing speed studied, and each spot's ratio of the intensities at 100% $N_2/O_2$ is displayed in a fashion where the chart represents the orientation of the spots on the slide.

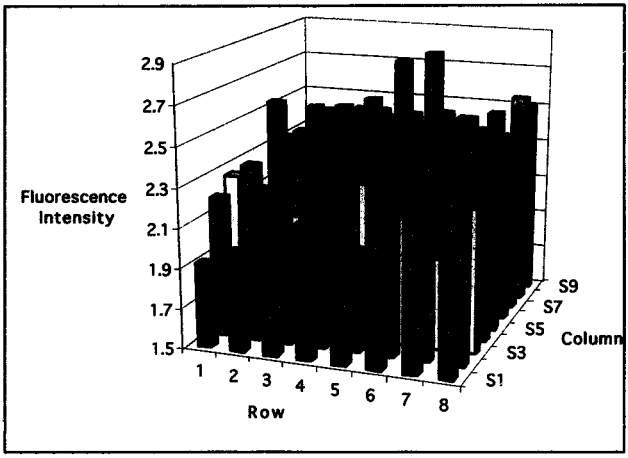


**Figure 24: 10-10ms Print Speed**

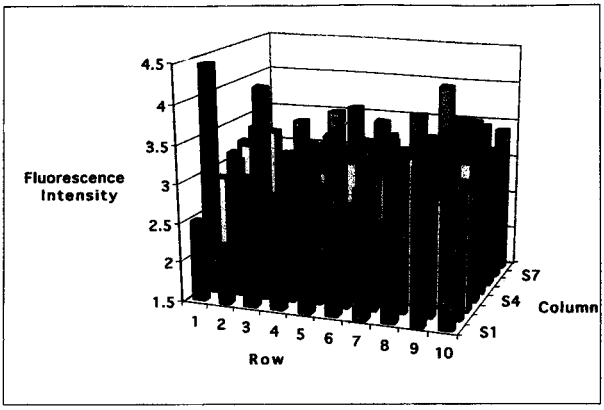


**Figure 25: 10-15ms Print Speed**

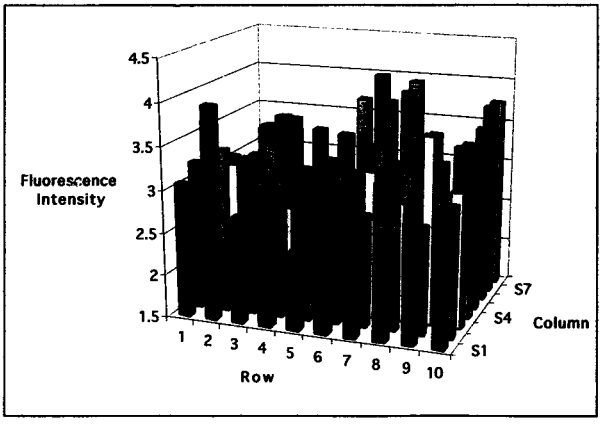


**Figure 26: 10-20ms Print Speed**

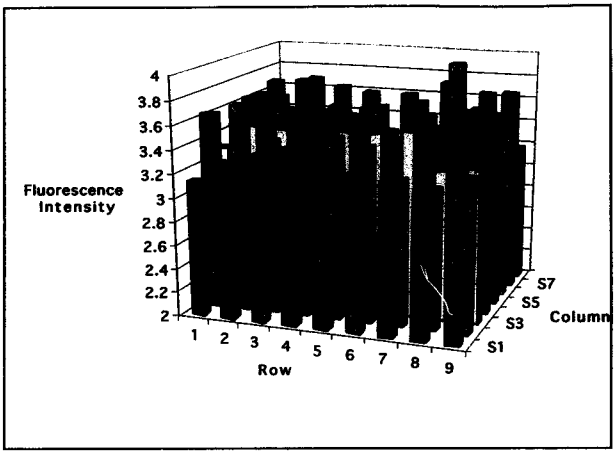


**Figure 27: 10-25ms Print Speed**

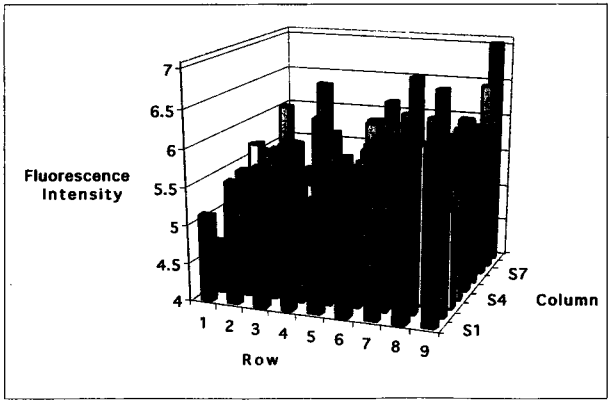


**Figure 28: 15-25ms Print Speed**

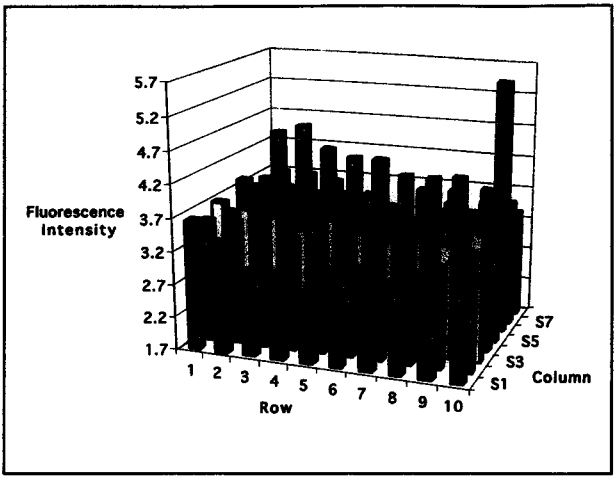


**Figure 29: 20-20ms Print Speed**

# PROJECT I
# CHAPTER 3:
# DISCUSSION

# Chapter 3: Discussion

## A. APTES Experiments

Based on the response profiles of the sol-gel microarrays printed on the APTES-treated slides and the overall appearance of the spots composing the microarray, it was apparent that slide pre-treatment with APTES yielded superior microarrays.

APTES provides the user with a molecule that has both a polar and a nonpolar component to it. This allows the highly polar sol-gel to effectively cling to the slide. The slide pre-treatment material is not so polar that the sol-gel spot will spread out too much and run into other spots, making them impossible to reproduce. Nor is this pre-treatment material so nonpolar that it causes the sol-gel to become repelled by the surface of the slide and bead up into a tiny spot that is too highly concentrated with sensing material in the middle of the spot. This makes the spots less reproducible. It also makes them much more structurally fragile and not well-attached to the slide [13].

Although APTES pre-treatment yields slides on which sol-gel microarrays can be printed reproducibly, there is a downside to it. Pre-treatment is highly time-consuming, as it requires a significant amount of sample preparation, and until we received the device that allowed us to treat 20 slides at once, only two slides could be treated at one time in one beaker. The APTES slides must sit in solution for 24 hours with a constant flow of argon gas passing through a sealed container, and then they must have a number of successive washings with methanol, chloroform and acetone. This is in comparison to the slides pre-treated with 1M NaOH, which require only 20 minutes to treat. When comparing the two methods of pre-treatment, it is apparent that the APTES pre-treatment

requires significantly more time and effort. It is also significantly more expensive, as it requires the purchase of APTES and generates a substantial amount of waste.

## B. Print Speed, Drying Temperature and Spin Coating Experiments

By viewing the data from this set of experiments, one can easily conclude that the optimal printing conditions for the sol-gel microarrays employed were a print speed of 10-25ms, drying at room temperature and no sol-gel spin coating on top of the spots, Array #5. This particular combination of variables gave the most reproducible microarray of spots. They also produced superior response times to changes in concentrations of nitrogen and oxygen gases in the chamber holding the slide pinprinted with the spots.

Indeed, of the four print speeds used, 10-25ms was the only speed that yielded useable data. 5-5ms and 5-10ms were so slow that the spots were not even round, they were rectangular. In addition to this, the actual printing process was very slow. Between the time printing the first spot and the last spot on the microarray, the spots would either grow significantly smaller by the end of the microarray, sometimes to the point of nonexistence, or the pin would clog due to the increased viscosity of the sol-gel as it evolved over time. 25-50ms was very fast, and the needle was in contact with the slide for so long that too much of the sol-gel was deposited in one spot that it spread out extensively and ran into other spots, making it impossible to ascertain the fluorescence intensity of one individual spot.

Although drying the microarrays at 4°C once they had been printed did not effect their spot-to-spot reproducibility, it did, for some reason, quench the fluorescence of the $Ru(dpp)_3^{2+}$, making it harder to distinguish the differences between the microarrays at 100% $N_2$ and 100% $O_2$.

The spin-coating of a layer of sol-gel on top of the microarrays, did, in fact, prevent the cracking, that was seen in the sol-gels without the spin-coating over them. However, the spin-coating seriously hindered the microarray's sensing capabilities, as seen from the data, specifically Figures 19-23. Spin-coating not only lengthened the response time of the Ruthenium sensor, but it adversely changed the size in the difference in signal between the fluorescence at 100% $N_2$ and the fluorescence at 100% $O_2$. In the microarrays without the spin-coating, the response time of the Ruthenium complex to changes in Nitrogen and Oxygen concentration was on the order of a couple of seconds. However, in the microarrays with the spin-coating, the response time was on the order of several minutes.

The nitrogen and oxygen gases not only had to disperse through the sol-gel matrix of spots on the microarray, but it also had to infiltrate the sol-gel matrix of the spin-coating on top of the microarray. Thus, the gases were not even in direct contact with the microarray, and thus, the ruthenium complex. Instead, they had to penetrate a barrier, and then effect the fluorescence changes in the $Ru(dpp)_3^{2+}$. Therefore, although the spin-coating does temporarily prevent cracking within the matrices of the sol-gel microarrays, it very drastically increases the response time of the sensor.

## C. Print Speed Experiments

Based on the data that was obtained from this set of experiments, one can conclude that the optimal print speed for n-propyl TMOS/ TMOS sol-gels is 10-25ms, as this gave the lowest relative standard deviation (5%) for spot-to-spot reproducibility. The spots are relatively uniform in size, shape and composition.

We concluded that this print speed should be employed when using n-propyl TMOS/ TMOS as the precursor and allowing the solution to hydrolyze for one hour. However, if the precursor is changed and the solution is allowed to hydrolyze for a different amount of time, then it is possible that another print speed should be used to accommodate for the difference in sol-gel composition and viscosity.

10-10ms, 15-25ms and 20-20ms print speeds also yielded low relative standard deviations for spot-to-spot reproducibility, between 8% and 9%. It is possible that these speeds can be used when pinprinting microarrays using sol-gels of different viscosities and compositions.

# PROJECT II:
## THE TESTING OF SOL-GEL PRECURSORS THROUGH THE USE OF FLUORESCENCE MEASUREMENTS OF EOSIN-Y.

# PROJECT II
# CHAPTER 1:
## EXPERIMENTAL

# Chapter 1: Experimental

## A. The Testing of Various Sol-Gel Precursors

The following chemicals and instruments were employed in this particular set of experiments:

| |
|---|
| Tetramethoxysilane, Aldrich Chemicals |
| Tetraethoxysilane, Aldrich Chemicals |
| n-Propyl Trimethoxysilane, Aldrich Chemicals |
| Methyl Trimethoxysilane, Aldrich Chemicals |
| Phenyl Triethoxysilane, Aldrich Chemicals |
| Absolute Ethanol |
| Deionized Water |
| 1M HCl stock solution |
| 5.0 x $10^{-6}$M Eosin-Y stock solution |
| Magnetic Stirring Plate |
| Polystyrene Fluorescence Cuvettes |
| Quantamaster Fluorometer |

Five possible precursors were used in this experiment in order to determine which of them most effectively encapsulated Eosin-Y. The five precursors were as follows:

- Tetramethoxysilane (TMOS)
- Tetraethoxysilane (TEOS)
- N-Propyl Trimethoxysilane (n-Propyl TMOS) + TMOS
- Methyl-Trimethoxysilane (Methyl TMOS) + TMOS
- Phenyl-Triethoxysilane (Phenyl TEOS) + TEOS

The recipe used to create the sol-gel monoliths was a 1:2:2:$10^{-4}$ molar ratio of sol-gel precursor: ethanol: water: 1 M HCl (catalyst). Enough solution was prepared to fill five 4-mL polystyrene cuvettes. The amount of each of the reactants needed to create each solution is found in Table 3.

| Sol-Gel Precursor | Precursor (mL) | Ethanol (mL) | Water (mL) | 1 M HCl (μL) |
|---|---|---|---|---|
| TMOS | 17.39 TMOS | 8.84 | 2.81 | 90 |
| TEOS | 17.39 TEOS | 8.84 | 2.81 | 90 |
| n-Propyl/TMOS | 8.70 TMOS | 8.84 | 2.81 | 90 |
| | 8.70 n-Propyl TMOS | | | |
| Methyl/ TMOS | 8.70 TMOS | 8.84 | 2.81 | 90 |
| | 8.70 Methyl TMOS | | | |
| Phenyl/ TEOS | 8.70 TEOS | 8.84 | 2.81 | 90 |
| | 8.70 Phenyl TEOS | | | |

**Table 3: Recipe for Each Sol-Gel Solution**

Each solution was made at room temperature, on different days, and the solutions were allowed to hydrolyze for approximately 1 hour or until the solution was monophasic. (The solutions are cloudy and heterogeneous upon mixing the reactants.) Once the solutions were monophasic, they were pipetted into polystyrene cuvettes (4 mL into each cuvette) and they were doped to the following concentrations with Eosin-Y:

- $5.0 \times 10^{-7}$ M
- $1.0 \times 10^{-6}$ M
- $1.5 \times 10^{-6}$ M
- $2.0 \times 10^{-6}$ M
- $2.5 \times 10^{-6}$ M

or, a 1:2:3:4:5 molar ratio of Eosin-Y from cuvette to cuvette. It is important to note that the concentration of Eosin-Y in the final monoliths is significantly larger than this because of the shrinking of the sol-gel solution. The monolith volume, however, was not measured and the final concentration of Eosin-Y is unknown. Consequently, the data will be presented using these initial concentrations.

These solutions were allowed to sit for about a week to let the hydrolysis reaction take place and for the solutions to shrink to monoliths so fluorescence analysis could take place. The cuvettes were placed in a covered styrofoam box at room temperature, and each individual cuvette was covered with a cuvette cover, as well.

Over the course of the polycondensation reaction, the monoliths were analyzed in the fluorometer in order to determine if the entrapped Eosin-Y was fluorescing and to see if they were following a plot where fluorescence intensity is linearly proportional to the concentration of encapsulated Eosin-Y.

It was determined after a week that the reaction was proceeding a bit slower than anticipated, so more catalyst was added to each of the cuvettes (20 µL of 1 M HCl), and the individual cuvettes were uncovered in order to allow some of the ethanol to evaporate. After another week, monoliths had formed in each of the cuvettes, and fluorescence measurements on the monoliths were performed.

An emission spectrum for each monolith was taken, and the settings were as follows for every monolith:

- Excitation Wavelength: 515 nm
- Emission Wavelength: 525-600 nm
- Excitation Slits: 3 nm
- Emission Slits: 3 nm
- 1 nm count/second

Once the fluorescence measurements had been performed to determine whether or not the fluorescence intensity of the doped gels adhered to linearity with the concentration of Eosin-Y, the sensing capabilities of each monolith were individually

tested using fluorescence measurements. The excitation and emission wavelengths were set to the values given above and aliquots of HCl and NaOH were added. A series of emission spectra were taken over time in order to determine the response time of the Eosin-Y doped monoliths to the resulting changes in pH.

To change the pH of the monolith, the gel would have to be placed in an aqueous solution. However, from experience, it was known that simply adding water to the cuvette holding the monolith would cause the monolith to shatter and thus render it useless for fluorescence measurements.

Natasha Eckert, Union College Class of 2002, developed a method to place the monoliths in an aqueous environment without shattering them. The uncovered monoliths were placed in a 250-mL beaker with roughly 50 mL of water in it, and the beaker was covered with parafilm for 2-3 days. This allowed the monolith to be accustomed to an aqueous environment via evaporation and condensation of the water from the beaker to the cuvette, and when water was added directly to the monolith, it did not shatter. This method was successful each time it was employed.

The following procedure was employed in order to test the sensing capabilities of each monolith. Once the monolith was placed in its aqueous environment, an emission spectrum was taken in the fluorometer using the same settings previously. Then, without removing the cuvette from its holder in the fluorometer, 200 μL of 1-M HCl was added to the cuvette. Subsequent fluorescence readings were taken at varying intervals for each monolith, depending on how quickly the fluorescence of the Eosin-Y in each one was diminished as a result of increasing acid concentration. However, the time intervals between each reading were on the scale of 1-3 minutes.

By the time the reversibility of the sensing capabilities of the monoliths could be tested, the gels were badly cracked, because they had been sitting in aqueous solution for over two months. Accurate fluorescence measurements could not be taken as a result. Therefore, a new set of monoliths was prepared.

All of the precursors listed in Table 3 were used in this procedure except for the phenyl TEOS/ TEOS combination, since the previously made monoliths produced unusable fluorescence data because of extensive cracking within the monolith. The same recipes were used as before, except less ethanol was added in hopes of making these monoliths slightly larger than the old ones. Ethanol is produced by the reaction in large quantities. By using less ethanol in the recipe, it should increase the amounts of precursor and water used, and subsequently produce more sol-gel.

Five cuvettes were used for each combination of precursors, and each cuvette held 4.0 mL of the gel. The following amounts of $5.0 \times 10^{-5}$ M Eosin-Y were added to the cuvettes: 10 μL, 15 μL, 20 μL, 25 μL and 30 μL. The gels in the cuvettes were allowed to dry and form into monoliths. An emission spectrum of each monolith was taken, and the same parameters previously listed were employed.

A procedure identical to the one described earlier was employed in order to introduce the monoliths into an aqueous environment. Since it was known from previous experimental data that all of these precursors were suitable platforms for pH sensors, 200 μL of 1-M HCl was added to each of the cuvettes with the knowledge that the HCl would decrease the fluorescence of the Eosin-Y. During the addition of the HCl, the cuvette remained in its holder in the fluorometer so the same part of the monolith was analyzed in subsequent emission spectra. After 20 minutes had elapsed, enough time for

the acid to diffuse fully into the monolith and decrease the fluorescence of the Eosin-Y, another emission spectrum was taken to assure that the acid-base reaction had, in fact, taken place.

In order to determine whether or not these sensors were reversible, and if they were, to what extent, 200 μL of 1-M NaOH was added at this point, and emission spectra were taken every couple of minutes until the fluorescence emission intensity at the peak wavelength had leveled off.

## B. Eosin-Y Experiments

The sensing capabilities of Eosin-Y in different solvents were tested in order to observe the behavior of the fluorescence spectra of Eosin-Y when it is in a solution.

Ten solutions were made, five with water as the solvent and five with a 1:1 ratio of water: ethanol as the solvent in the polystyrene fluorescence cuvettes. The following amounts of $5.0 \times 10^{-5}$ M Eosin-Y stock solution were added to each of the solutions: 10 μL, 15 μL, 20 μL, 25 μL and 30 μL.

Following the addition of Eosin-Y, a fluorescence spectrum was taken of each cuvette, and the following procedure was used to assess the sensing capability and the reversibility of the sensing capability of Eosin-Y at varying concentrations and in two different solvents.

100 μL of 0.1-M HCl was added to the cuvette while it was still in the cuvette holder in the fluorometer and an emission spectrum was taken immediately. Once the acid had decreased the fluorescence of the Eosin-Y and a reading had been taken to determine that the fluorescence had, in fact, decreased (this only took about a minute), 100 μL of 0.1-M NaOH was added to test whether that the sensing capabilities of the Eosin-Y were reversible.

After the addition of NaOH, an emission spectrum was taken to observe that the fluorescence had, in fact, increased even higher than its initial peak fluorescence in many of the cases. After the emission spectrum had been taken, another 100 μL of 0.1 M-HCl was added to determine if the fluorescence could be decreased again, and another

emission spectrum was taken. This procedure was followed for all of the Eosin-Y solutions.

It was observed during these investigations that there were significant wavelength shifts in the spectrum of the Eosin-Y at different solvent compositions. These wavelength shifts appear to be caused by different polarities of the solvents interacting with the Eosin-Y.

As a result of this observation, experiments were performed in order to determine whether or not polarity of the solvent was the cause of the wavelength shift. The first procedure employed was to make twelve Eosin-Y solutions: three in water, three in a 50/50 volumetric ratio of ethanol/water, three in ethanol, and three in 1-propanol, in decreasing degrees of polarities. 4 mL of each of these solvents was pipetted into a cuvette, and the following amounts of $5.0 \times 10^{-5}$ M Eosin-Y were added to each of the cuvettes of each set of solvents: 5 μL, 10 μL and 15 μL.

The same procedure described above was used to add the HCl and NaOH to look at the sensing capabilities of the Eosin-Y in each solvent, except closer attention was given to the peak wavelength of the fluorescence emission.

After these experiments, it was noted that the polarity of a solvent was affecting the emission spectra of the Eosin-Y somewhat; however, as Eosin-Y in 1-propanol gave essentially the same spectra as Eosin-Y in ethanol. The observed behavior of Eosin-Y in water and Eosin-Y in ethanol still differed significantly, and the next set of experiments explores this behavior.

Eleven different solutions were placed polystyrene cuvettes. Each solution contained the same amount of Eosin-Y, but all the solutions varied in their solvent composition. Table 4 outlines the solvent composition of each of the solutions:

| Solution | % Water by Volume | % Ethanol by Volume |
|---|---|---|
| 1 | 0 | 100 |
| 2 | 10 | 90 |
| 3 | 20 | 80 |
| 4 | 30 | 70 |
| 5 | 40 | 60 |
| 6 | 50 | 50 |
| 7 | 60 | 40 |
| 8 | 70 | 30 |
| 9 | 80 | 20 |
| 10 | 90 | 10 |
| 11 | 100 | 0 |

**Table 4: Outline of Solvent Composition for Eosin-Y Behavior Experiments**

After 20 μL of 5.0 x $10^{-5}$ M Eosin-Y was added to the cuvettes, each cuvette was shaken vigorously in order to assure that the Eosin-Y was properly mixed into the solvent.

An emission spectrum was taken of each solution, and the peak wavelength and intensity was noted for each.

# PROJECT II
# CHAPTER 2:
# RESULTS

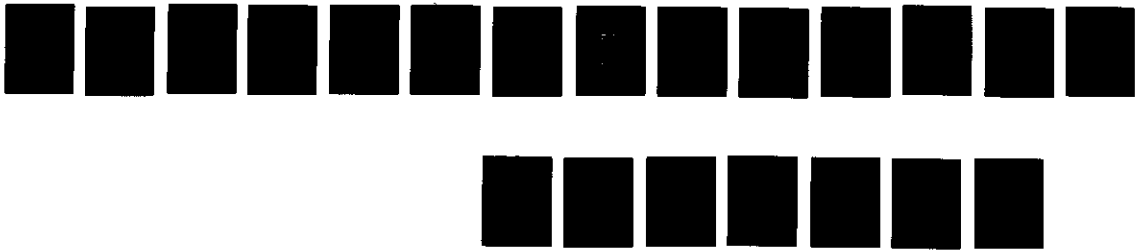

## Chapter 2: Results

### A. The Testing of Various Sol-Gel Precursors

All of the sol-gel precursors did follow a linear trend when the results of Fluorescence Intensity versus Concentration of Eosin-Y were plotted. Figures 30, 31, 32, 33, and 34 illustrate the emission spectra of Eosin-Y at varying concentrations in the five different precursors after they have formed into gels. Figure 35 illustrates the plots of fluorescence intensity v. concentration of entrapped Eosin-Y for TMOS, n-propyl TMOS/ TMOS, methyl TMOS/ TMOS and phenyl TEOS/ TEOS doped with different concentrations of Eosin-Y. TEOS is not included because the Eosin-Y-doped monoliths prepared from TEOS did not exhibit a linear trend for fluorescence intensity as a function of concentration of Eosin-Y.

| Color Key for Figures 30-34 : Concentration of Eosin-Y | |
|---|---|
| Blue: $2.5 \times 10^{-6}$M | Red: $2.0 \times 10^{-6}$M |
| Green: $1.5 \times 10^{-6}$M | : $1.0 \times 10^{-6}$M |
| Purple: $5.0 \times 10^{-7}$M | |

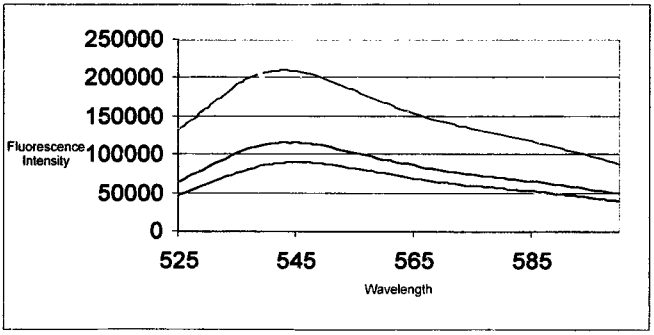


**Figure 30: Fluorescence Intensity of TEOS Sol-Gels Doped with Eosin-Y**

**Key of Colors for Figures 30-34 : Concentration of Eosin-Y**

Blue: 2.5 x $10^{-6}$M
Red: 2.0 x $10^{-6}$M
Green: 1.5 x $10^{-6}$M
: 1.0 x $10^{-6}$M
Purple: 5.0 x $10^{-7}$M

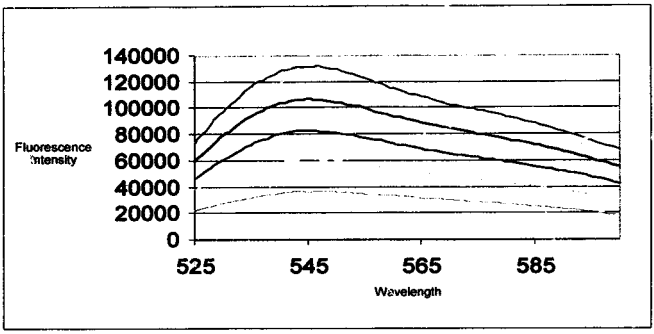


**Figure 31: Fluorescence Intensity of TMOS Sol-Gels Doped with Eosin-Y**

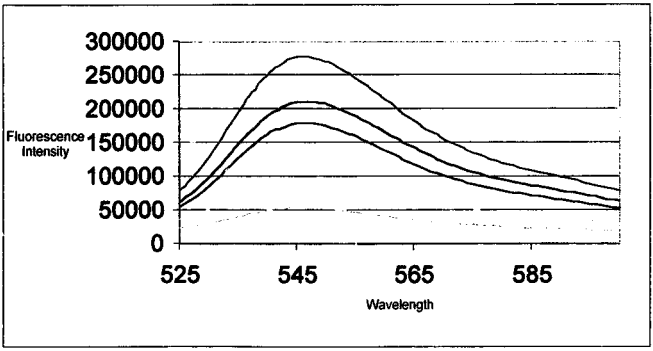


**Figure 32: Fluorescence Intensity of n-Propyl TMOS/ TMOS Sol-Gels Doped with Eosin-Y**

**Key of Colors for Figures 30-34 : Concentration of Eosin-Y**

Blue: 2.5 x $10^{-6}$M Red: 2.0 x $10^{-6}$M

Green: 1.5 x $10^{-6}$M : 1.0 x $10^{-6}$M

Purple: 5.0 x $10^{-7}$M

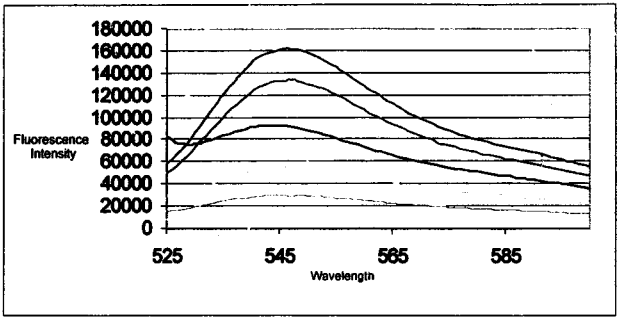


**Figure 33: Fluorescence Intensity of Methyl TMOS/ TMOS Sol-Gels Doped with Eosin-Y**

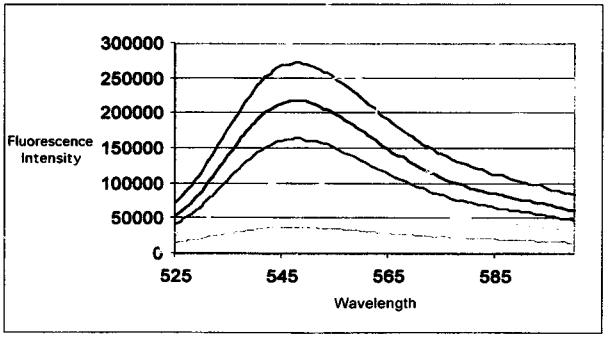


**Figure 34: Fluorescence Intensity of Phenyl TEOS/ TEOS Sol-Gels Doped with Eosin-Y**

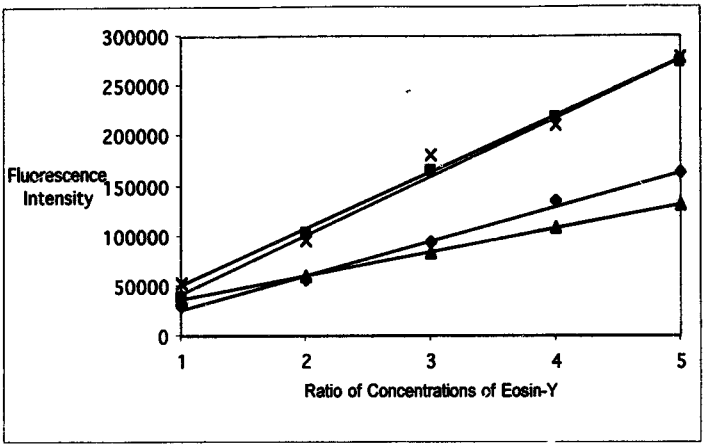


**Figure 35: Fluorescence Intensity v. Concentration of Encapsulated Eosin-Y for Four of the Five Precursors**

**× = TMOS**
**■ = Phenyl TEOS/ TEOS**
**◆ = Methyl TMOS/ TMOS**
**▲ = n-Propyl TMOS/ TMOS**

Table 4 gives each of the $R^2$ (R-squared) values for the plots of fluorescence v. concentration of Eosin-Y in each of the five precursors. The $R^2$ value assesses the adherence of the plot to linearity. As the $R^2$ value grows closer and closer to 1.000, the more tightly the plot is adhering to linearity, and the more consistently that particular sol-gel precursor has encapsulated the Eosin-Y.

| Precursor | R-squared value |
|---|---|
| TEOS | 0.6350 |
| TMOS | 0.9853 |
| Methyl TMOS/ TMOS | 0.9943 |
| Phenyl TEOS/ TEOS | 0.9982 |
| n-Propyl TMOS/ TMOS | 0.9998 |

**Table 5: $R^2$ Values of the Plots of Fluorescence Intensity Versus Concentration of Eosin-Y in each of the Precursors**

The shape and stability of the monoliths were observed as groups of particular precursors, and the following observations were made:

TMOS Monoliths: These monoliths were cracked substantially, which may affect their emission spectra, depending on where the excitation light penetrates the monolith. They did, however, pull away from the walls of the cuvette nicely, and without clinging to them.

TEOS Monoliths: Although the bodies of the monoliths did not crack as much as the TMOS ones did, these monoliths clung heavily to the walls of the cuvette. Once they had shrunk, they left a large amount of residue on the cuvette walls, sol-gel that had not shrunk with the monolith. This is most likely the reason for poor linearity in the plots of fluorescence intensity versus concentration of Eosin-Y.

n-Propyl TMOS/ TMOS Monoliths: These monoliths were, by far, the cleanest monoliths in terms of cracking, as they did not exhibit any significant amount of cracking within the body of the monolith. However, these monoliths took the longest amount of time to pull away from the walls of the cuvette.

Phenyl TEOS/ TEOS Monoliths: These sol-gels took the longest amount of time to solidify, and form the desired monolith. However, upon forming a monolith, each of the gels immediately shattered, rendering them useless in subsequent fluorescence emission measurements, as the shattered glass scattered the excitation beam. These gels were then deemed unsuitable for the encapsulation of Eosin-Y.

Methyl TMOS/ TMOS Monoliths: Each of these monoliths exhibited a large meniscus in its respective cuvette. Due to this meniscus, a couple of the monoliths have a large crack extending from the valley of the meniscus to the bottom of the cuvette where the monolith rests. There was no sol-gel coating on the inside of the cuvettes despite the large meniscus.

Each of the precursor monoliths had different response times to the quenching of the fluorescence of the Eosin-Y by 1 M HCl. This is due to the fact that some of the gels were more cracked than others, and some of the monoliths had pulled farther away from the walls of the cuvette than others had. Thus, the HCl could infiltrate cracks in the body of the monolith more easily than it could penetrate pores in the body of the monolith and the response time is quicker for fragmented monoliths.

Figures 36, 37, 38 and 39 show the response of the monoliths, grouped together by precursor used, once 200 μL of 0.1 M HCl was added to each of the monoliths in an aqueous environment at t=0 seconds. Notice that the phenyl TEOS/TEOS precursor is not included in this set of data, as the extensive shattering of the glass yielded unusable data for this set of experiments.

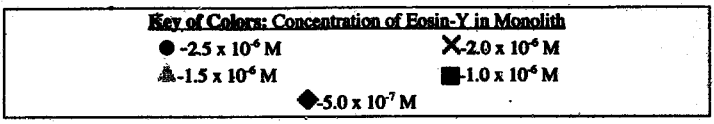


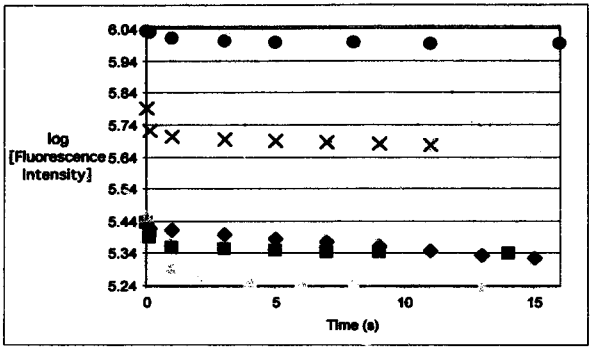


**Figure 36: Response of TMOS Monoliths to HCl Addition**

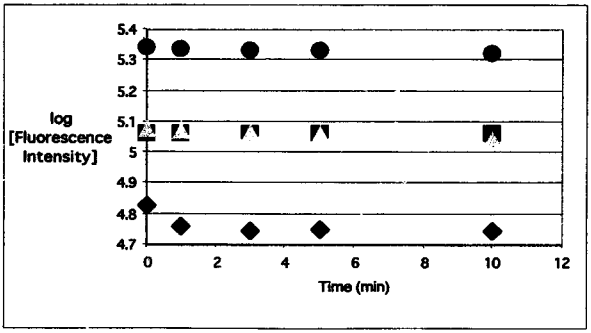


**Figure 37: Response of TEOS Monoliths to HCl Addition**

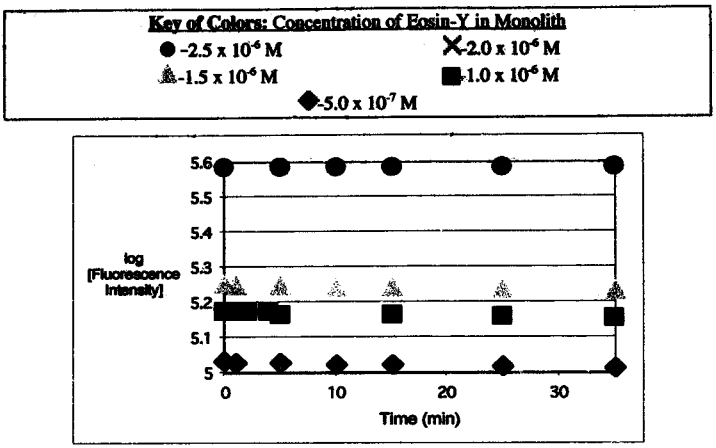


**Figure 38: Response of n-Propyl TMOS Monoliths to HCl Addition**

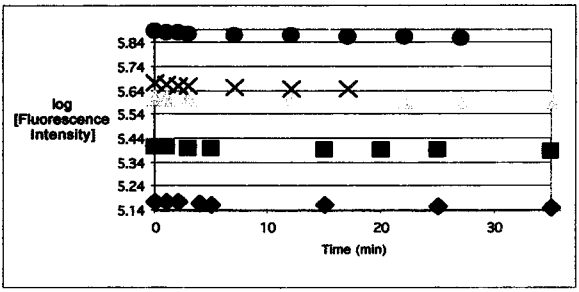


**Figure 39: Response of Methyl TMOS Monoliths to HCl Addition**

In Figures 40 and 41, the responses of the sol-gel monoliths to NaOH addition are shown. It was determined that in these monoliths, there was over 100% reversibility of the sensors in every case. The initial fluorescence was measured without the addition of any acid or base, and then 200 μL of 0.1 M HCl was added to the cuvette at t=0 seconds, and it was allowed to sit for 20 minutes. The fluorescence was again measured, and then 200 μL of 0.1 M NaOH was added to the cuvette. In every monolith, the sensor obtained over 100% reversibility within less than 10 minutes, and by the end of 20 minutes, the sensors had reached, in some cases, fluorescence signals more than 300% of the original intensities.

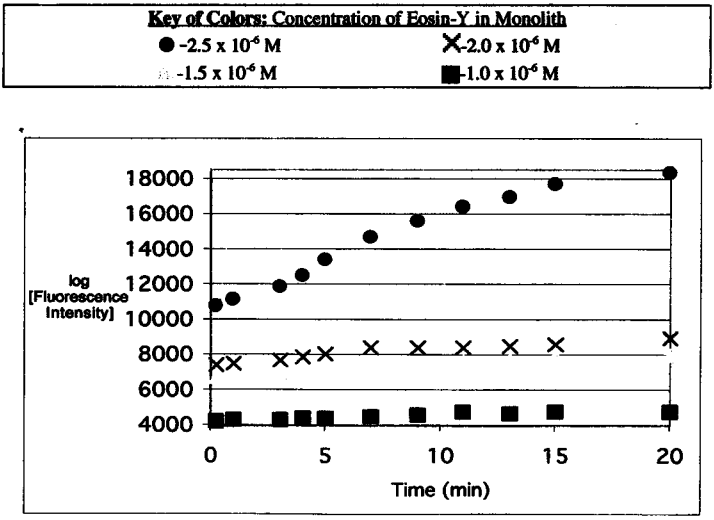


**Figure 40: Response of TEOS Monoliths to NaOH Addition**

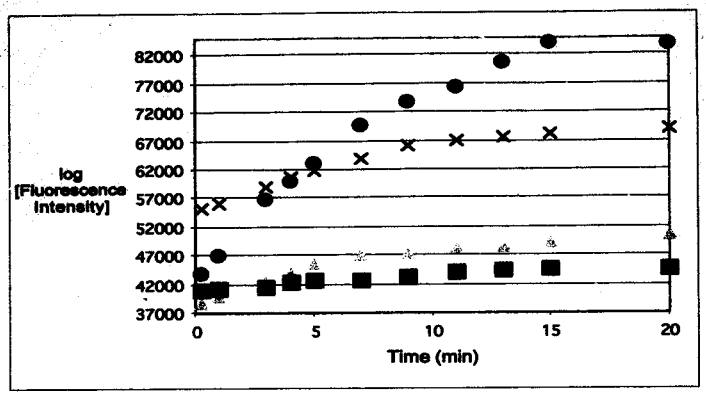


**Figure 41: Response Time of TMOS Monoliths to NaOH Addition**

## B. Eosin-Y Experiments

There were a number of differences between the solutions of Eosin-Y in water and Eosin-Y in ethanol. The solution of Eosin-Y in water was orange-colored, whereas the solution of Eosin-Y in ethanol was pink and had bubbles. It was hypothesized that these differences in color in the two solutions, and therefore, in their absorption spectra would ultimately lead to differences in the emission spectra between the different solutions.

When HCl and NaOH were added to the solutions and the response time was tested using the fluorometer, the response was much quicker than it was in the gels. This is because it is much easier for the acid and base to diffuse through the solutions than it is to diffuse through the solid Si-O matrix and react with the Eosin-Y. Therefore, a response time that would be on the order of 15 minutes for Eosin-Y in a gel is reduced to 5-10 seconds when the Eosin-Y is in solution.

Figure 42 illustrates the response of Eosin-Y in solution to acid and base. This test also verifies that the Eosin-Y is highly responsive to changes in pH, as 0.1 M HCl and 0.1 M NaOH were added to a solution with a concentration on the order of $10^{-6}$M Eosin–Y in 100 μL increments. These variations in pH ultimately led to highly significant changes in the fluorescence intensity emitted from the sample. The peaks in the chart indicate the response of the fluorescence of the Eosin-Y following the addition of NaOH, and the valleys in the chart indicate the response of the fluorescence of the Eosin-Y following the addition of HCl.

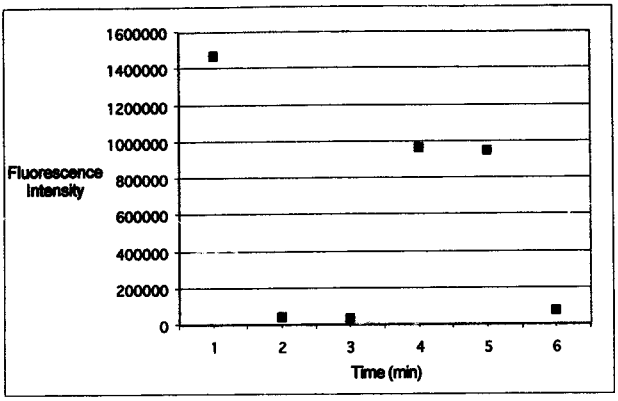


**Figure 42: Response of Eosin-Y in Solution when pH is Altered**
**HCl added at t=1, t=5**
**NaOH added at t=3**

It was also noted that when Eosin-Y was in water, it has a different emission spectrum from that of Eosin-Y in ethanol, as expected. When Eosin-Y is in water, its emission spectrum peaks at approximately 533 nm, but when Eosin-Y is in ethanol, its peak emission occurs at 540 nm.

In order to determine if this was due to polarity, Eosin-Y was dissolved in solutions of water, 1-propanol and ethanol and emission spectra of these solutions were taken. The water and the ethanol yielded the same results as seen before, and it was expected that the emission spectrum of the Eosin-Y in 1-propanol, the most nonpolar of the solvents used would peak at a higher wavelength than that for Eosin-Y in ethanol. The emission spectra of the Eosin-Y in 1-propanol did, in fact, peak at approximately 542nm, supporting the theory that the emission spectra of Eosin-Y could possibly be

dependent on the polarity of its solvent. However, since the emission and excitation slits were set at 3 nm, further work must be performed in order to determine if this wavelength shift was, in fact, significant.

According to Dunn and Zink [14], the association of specific spectral changes with hydrolysis and condensation reactions can establish whether or not these reactions are occurring and if they have reached a certain equilibrium solvent composition. This can then provide insight into the rates of these hydrolysis and polycondensation reactions.

As one can see from the results of the experiment where the solvent composition ratio of ethanol : water was varied and each was doped with the same concentration of Eosin-Y, there is a direct relationship between the peak of the emission spectra of these solutions and the ratio of water to ethanol. As seen in Figure 43, as the concentration of Ethanol increases in the solvent, the peak wavelength of the emission spectra increases as well. This is an indication that Eosin-Y could be applied to monitor the reaction rates of sol-gels up to approximately a 40:60 ratio of ethanol to water.

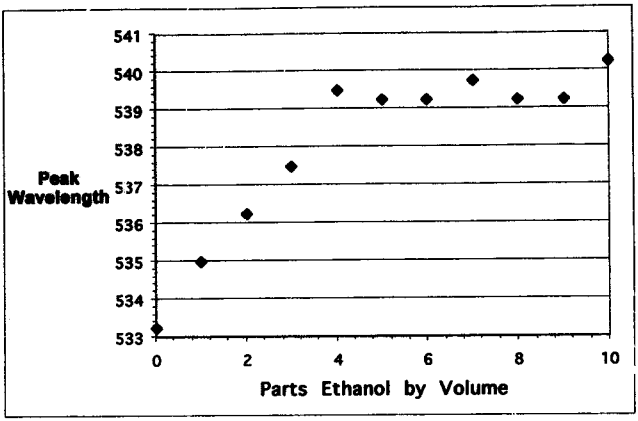


**Figure 43: Solvent Ratio of Water: Ethanol and its Effects on the Peak Wavelength of the Emission Spectra of Eosin-Y**

# PROJECT II
# CHAPTER 3:
# DISCUSSION

# Chapter 3: Discussion

## A. The Testing of Various Sol-Gel Precursors

Each of the precursors used had a number of advantages and disadvantages in the making of sol-gel monoliths. Although they did have some drawbacks, n-propyl TMOS/ TMOS and methyl TMOS/ TMOS appeared to be the superior precursor mixtures based on the data and observations obtained.

Sol-gels prepared from TEOS and TMOS without the addition of an ormosil derivative had the luxury of being easier to make, and the materials were less expensive to obtain than n-propyl TMOS, methyl TMOS and phenyl TEOS. These monoliths also responded very quickly to changes in pH. When HCl and NaOH were added to the aqueous solutions and allowed to react with the Eosin-Y encapsulated in the sol-gel matrix, and response times were on the order of 2-10 minutes. However, one of the drawbacks to using these particular precursors was that the monoliths were not aesthetically pleasing or as robust as the other monoliths. They cracked very easily. This affected the fluorescence spectra as a result of two things: (1) the excitation light scattering from the cracks in the glass and (2) changes in collected fluorescence intensity because of shifting in position of the sol-gel as it cracked. Consequently, they gave inferior calibration curves, as one can verify by viewing Table 5, where the $R^2$ values for each of the calibration curves for each set of monoliths are displayed. The $R^2$ values for TEOS and TMOS are significantly lower than those of n-propyl TMOS/ TMOS, methyl TMOS/ TMOS and phenyl TEOS/ TEOS.

n-Propyl TMOS/ TMOS yielded the best plot of fluorescence intensity versus concentration of Eosin-Y, with an $R^2$ value of 0.998. Moreover, these monoliths were

by far the most aesthetically pleasing. They experienced minimal cracking and as a result, are promising for use as a platform for Eosin-Y-doped sensors. The hydrolysis time for these sol-gels was also much shorter than that of the other sol-gels. n-Propyl TMOS/ TMOS sol-gels took approximately one hour to hydrolyze while the other precursors took approximately two hours.

However, there were some drawbacks to using n-propyl TMOS/ TMOS. n-Propyl TMOS is more expensive than TEOS and TMOS, so it had to be used sparingly. In addition to this, these monoliths took the longest time to pull away from the walls of the cuvettes, even though they did not take very long to form solids. The response time to changes in pH was significantly longer than that of the other monoliths. The HCl and NaOH took more time to diffuse through this Si-O matrix than in other monoliths consisting of smaller, cracked pieces. The monolith had also not completely pulled away from the wall of the cuvette at the time of the tests for sensing capabilities. Whereas the other monoliths of the same size took only 2-5 minutes to respond to the changes in pH, the n-Propyl TMOS/ TMOS monoliths took approximately 10-15 minutes to experience a maximum response.

Phenyl TEOS/ TEOS sol-gels had substantially more drawbacks than advantages and they proved to be highly inferior sensors for changes in pH through the encapsulation of Eosin-Y. The sole advantage of phenyl TEOS/ TEOS as a precursor was that it yielded a highly precise plot of fluorescence intensity v. concentration of Eosin-Y, giving an $R^2$ value of 0.9982. However, the phenyl TEOS/ TEOS presented a number of disadvantages. They took the longest amount of time to become solid monoliths, as they retained their liquid form for approximately three weeks, whereas the

other monoliths had formed solids after approximately two weeks. Once the phenyl TEOS/ TEOS sol-gels had formed monoliths, they retained their monolith form for only a short period of time. Approximately three days after these monoliths had begun to pull away from the walls of the cuvettes, they shattered so much that they were completely opaque and it was impossible for the excitation beam of the fluorometer to penetrate the cracked monoliths.

The methyl TMOS/ TMOS sol-gels had few disadvantages and a substantial number of advantages; they appear to be the superior sensors of the group of the precursors tested. The gels were highly aesthetically pleasing, and their only flaw was the large meniscus clinging to the walls of the cuvettes. This often caused a crack to form down the middle of the monolith, but if the excitation beam was positioned so that it was not diverted by this crack, then the emission spectra were not adversely affected. As a result of this, methyl TMOS/ TMOS sol-gels gave excellent fluorescence v. concentration plots, yielding an $R^2$ value of 0.9943.

The methyl TMOS/ TMOS precursors did not take a long time to form the desired solid monolith. Complete hydrolysis was on the order of two weeks. These monoliths also readily responded to changes in pH in a relatively short amount of time, comparable to the response times of TMOS and TEOS monoliths. They took approximately 8 minutes to respond to changes in pH, not quite as long as the n-propyl TMOS/ TMOS monoliths took to respond to the pH changes.

If the sol-gels are being used solely for sensing purposes, then the TEOS and TMOS sol-gels should be used, since they are the least expensive to make and they respond very quickly to changes in pH.

If a highly stable sol-gel with minimal cracking is desired, then n-propyl TMOS/ TMOS should be used, as these monoliths experienced almost no cracking within their matrices.

If both of these qualities in a sol-gel monolith are desired, then methyl TMOS/ TMOS should be used as a precursor. It yielded relatively aesthetically pleasing monoliths with small amount of cracking within the matrix of the sol-gel. The Eosin-Y encapsulated in this particular precursor also responded fairly quickly to the changes in pH.

## B. Eosin-Y Experiments

We can conclude that Eosin-Y is highly sensitive to slight changes in pH not only in aqueous solution but in the sol-gel solid matrix as well. The sol-gel matrix effectively encapsulates the Eosin-Y without altering its chemical composition significantly, proven by the response of the Eosin-Y to changes in pH of the sol-gel environment. Eosin-Y is, in fact, an effective sensor when combined with sol-gels.

It is apparent that more research must be performed in the area of the spectroscopic properties of Eosin-Y, as it exhibits a number of unique attributes that can be applied to the study of the reaction rates of sol-gels. The wavelength at which the peak fluorescence intensity is observed decreases as the amount of ethanol in the solution increases and the amount of water decreases. In principle, Eosin-Y fluorescence could therefore be applied to monitor the reaction rates of sol-gels. As the reaction progresses, the concentration of water in the solution decreases as it is employed into the reaction, and the concentration of ethanol increases since it is a by-product of the reaction. Spectral changes in entrapped Eosin-Y could be used to assess the concentrations of water and ethanol in the sol-gel over time. This information could be used to determine the rate of polycondensation in the sol-gel matrix.

## References


1) Lev, O.; Tsionsky, M.; Rabinovich, L.; Glezer, V.; Sampath, S.; Pankratov, I.; Gun, J. *Analytical Chemistry*, **1995**, 67, 22A-30A.

2) Narang, U.; Wang, R.; Prasad, P.N.; Bright, F.V. *Journal of Physical Chemistry*, **1994**, 98, 17-22.

3) Dave, B.C.; Dunn, B.; Selverstone Valentine, J.; Zink, J.I. *Analytical Chemistry*, **1994**, 66, 1120A-1126A.

4) Lobnik, A.; Oehme, I.; Murkovic, I.; Wolfbeis, O.S. *Analytica Chimica Acta*, **1998**, 367, 159-165.

5) McDonagh, C.; MacGraith, B.D.; McEvoy, A.K. *Analytical Chemistry*, **1998**, 70, 45-50.

6) Zaharescu, M.; Jitianu, A.; Badescu, V.; Radu, M. *Advances in Science and Technology*, **1999**, 15, 150-158.

7) Keeling-Tucker, T.; Brennan, J.D. *Chemical Meterials*, **2001**, 13, 3331-3350.

8) *Principles of Fluorescence Spectroscopy*; Lakowicz, J.R.; University of Maryland School of Medicine; Baltimore, Maryland, 1983; p.4.

9) Okamoto, K.; Taniguchi, T.; Takahashi, M.; Yamagishi, A. *Langmuir*, **2001**, 17, 195-201.

10) *The Sigma-Aldrich Handbook of Stains, Dyes and Indicators*; Green, F.J.; Aldrich Chemical Co. Inc.: Milwaukee, Wisconsin, 1991; pp. 304-305.

11) Valeur, B.; Badaoui, F.; Bardez, E.; Bourson, J.; Boutin, P.; Chatelain, A.; Devol, I.; Larrey, B.; Lefevre, J.P. *Chemosensors of Ion and Molecule Recognition*, **1997**, 195-220.

12) Lu, B.; Xie, J.; Lu, C.; Wu, C.; Wei, Y. *Analytical Chemistry*, 1995, 67, 83-87.

13) Bright Lab, SUNY Buffalo, Personal Communication

14) Dunn, B.; Zink, J.I. *Chemical Materials*, **1997**, 9, 2280-2291.